

M. Faverzani¹ · P. Day² · A. Nucciotti¹ · E. Ferri¹

Developments of Microresonators Detectors for Neutrino Physics in Milano

31.07.2011

Keywords MKID

Abstract Superconducting microwave microresonators are low temperature detectors which are compatible with large-scale multiplexed frequency domain read-out. We aim to adapt and further advance the technology of microresonator detectors to develop new devices applied to the problem of measuring the neutrino mass. More specifically, we aim to develop detector arrays for calorimetric measurement of the energy spectra of ^{163}Ho EC decay ($Q \sim 2\text{-}3$ keV) for a direct measurement of the neutrino mass. In order to achieve these goal, we need to find the best design and materials for the detectors. A recent advance in microwave microresonator technology was the discovery that some metal nitrides, such as TiN, possess properties consistent with very high detector sensitivity. We plan to investigate nitrides of higher-Z materials, for example TaN and HfN, that are appropriate for containing the energy of keV decay events, exploring the properties relevant to our detectors, such as quality factor, penetration depth and recombination time.

1 Introduction

The potential of low temperature detectors for applications requiring very high sensitivity was realized 50 years ago with the introduction of cryogenic bolometers using semiconducting thermistors¹. Since then several improvements were made: in the early 1990s, the millimetre wavelength "spider-web" bolometer was introduced² making it possible to achieve background limited performance (BLIP). At this point, the only way to improve the overall sensitivity of an instrument is to increase the number of detectors. A practical difficulty arises, however, in

1:Università di Milano Bicocca and INFN Milano Bicocca Tel.:+39 0264482341 E-mail: marco.faverzani@mib.infn.it

2: Jet Propulsion Laboratory, Pasadena, CA, U.S.A.

extending the semiconducting bolometer/calorimeter technology to larger arrays: the JFET amplifiers used with these devices operate at around 120K, much higher than the detector temperature of one to three hundred millikelvin. Running individual wiring between the two temperature stages is impractical for array sizes of more than a few hundred. Progress toward larger arrays has been made with the introduction of superconducting detectors. While the number of detectors per output channel, termed multiplexing factor, is so far limited to 32 by the (few MHz) bandwidth of the SQUID array amplifier, this technology has enabled the current generation of instruments with a few thousands of detectors.

A new direction in the field was introduced with the demonstration of a different superconducting detector based on a superconducting microresonator in 2003³. The microresonators respond to absorbed radiation by changing their surface impedance, which is reflected as changes in resonant frequency and the Q-factor. As the detectors are well matched to low-noise cryogenic microwave amplifiers, such as HEMTs, which have multi-GHz bandwidth, multiplexing factors of thousands are theoretically possible. The operating principle of the microresonator detector arrays that we will develop is shown in fig.1. Absorption of energy in a superconductor leads to the breaking of Cooper pairs and the creation of quasiparticle excitations, as long as the energy of the quanta absorbed exceeds the gap energy of the superconductor, $h\nu \gtrsim 2\Delta \sim 3.5 k_b T_c \sim \text{meV}$. A keV scale X-ray photon will produce millions of quasiparticles in a typical superconducting film. Because a fraction of the energy is lost to low energy phonons, the quasiparticle production varies statistically, leading to a theoretical resolution $R \sim (10^6)^{1/2} = 1000$ or $\Delta E \sim 1\text{eV}$ for keV X-rays. In order to achieve such resolution, the number of quasiparticles produced must be accurately measured. According to the Mattis-Bardeen theory, quasiparticles perturb the complex conductivity, $\sigma_1 - i\sigma_2$, of the superconductor. The resulting perturbation $\delta\sigma$ may be accurately measured through vector microwave measurements of lithographed microresonators. Changes in σ_2 produce an inductive response of a microresonator, manifested as a frequency change, while changes in σ_1 produce a dissipative response, observed as a change in Q. When operating in a pulse detection mode, such as for X-ray detection, the signal power is at high enough frequencies so that the greater inductive response is close to compensated by the $1/f^{1/2}$ frequency noise when compared to the dissipative signal, so it is beneficial to include both signals in the readout⁴. Large arrays of these detectors can be read out efficiently by giving each microresonator a different frequency (fig.1-right). Due to this straightforward readout scheme, rapid progress is being made toward developing large arrays for astronomy.

2 Microresonator Detectors for Neutrino Physics in Milano

Measurement of the mass of the neutrino, the lightest of the fundamental particles, has been an outstanding issue for many years; today neutrinos are known to have non-zero mass from recent observations of oscillations between neutrino types. These kind of experiment, though, aren't able to measure the exact mass values, which are still unknown. One type of experiments which can tackle directly these issue without model dependences are direct kinematic studies of a low energy nuclear decay involving the production of a neutrino, where the shape

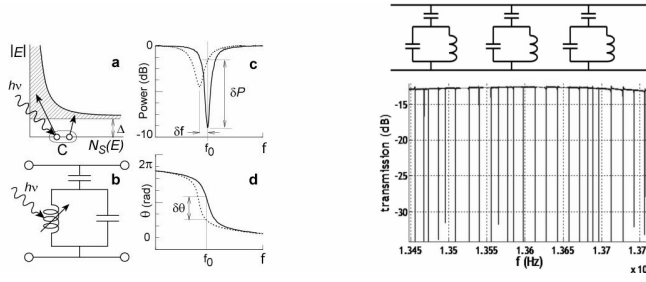


Fig. 1 Left: Photon or phonon energy absorbed in a superconductor creates quasiparticles that change the surface impedance and cause perturbations in the frequency and quality factor (dissipation) of a superconducting microresonator. **Right:** A series of microresonators with slightly different frequencies is arrayed along a single microwave transmission line.

of the decay energy spectrum near its endpoint provides the neutrino mass. The beta decay of ^{187}Re and the electron capture decay of ^{163}Ho are being considered for MARE experiment⁵. Our main target is the development of athermal detectors for an electron-capture decay endpoint measurement of the neutrino mass using Holmium as the source material. The density of the holmium can be adjusted to produce a desired count rate. Approximately 3×10^{12} ^{163}Ho nuclei are needed for a count rate of 10Hz. For an implanted area of $3\mu\text{m} \times 500\mu\text{m}$, we need only 2×10^{17} atoms/cm², which should be straightforward to achieve. Before implanting the ^{163}Ho nuclei, the devices will be characterized using low energy X-ray sources to irradiate the sensitive area. The fundamental noise of a pair-breaking detector for phonon counting applications is set by the statistics of the energy cascade process that produces quasiparticles and low energy phonons. If we tune the T_c of our sensor material to be 1K, and assuming a typical conversion efficiency of 0.5, we expect for a 2 keV decay event an energy resolution $\Delta E \sim 0.8$ eV. The theoretical energy resolution will actually be slightly better than this because the Fano factor, $f < 1$.

2.1 Resonator geometry

Consider a simple detector design (fig.2): the “lumped-element” resonators consist of two interdigital capacitors (IDC) connected with a coplanar strips (CPS) transmission line. The resonator is capacitively coupled on one side to a coplanar waveguide (CPW) line that is used for the readout. The strength of the coupling, which sets the coupling quality factor Q_c , is determined by the width of the gap between the CPW line and the resonator. The spacing and width of the conductors of the IDCs is $30\mu\text{m}$. This large spacing is intended to reduce two-level systems (TLS) noise associated with amorphous dielectric layers at surfaces by decreasing the surface layer to volume ratio of the capacitors. This structure was the subject of a simulation with Sonnet software, in order to determine the resonance frequency and the dependence of Q_c on the width of the coupling gap. A superconducting film with thickness t that is thin compared to a penetration depth can be modeled in Sonnet by specifying a surface inductance L_s . Even though in our case we are

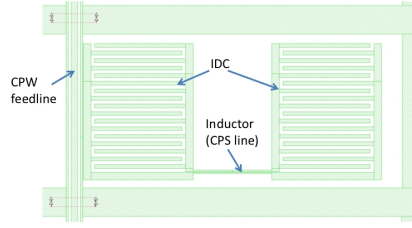


Fig. 2 Concept for the microresonator array approach to the internal source spectral endpoint neutrino mass experiment. Each resonator consists of an approximately mm^2 area interdigital capacitor connected to an inductive section with a CPW transmission line geometry. The center conductor of the CPW is made of TaN or another nitride material with large kinetic inductance and is the host to the implanted holmium atoms.

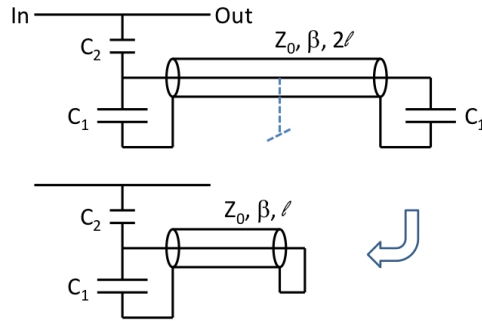


Fig. 3 Circuit model representation of the resonator. Because of the virtual ground in the center of the transmission line, we can simplify the circuit as shown below.

not strictly in the thin film limit, the description of the film in terms of L_s should still be quite accurate. For arbitrary film thickness the relation between penetration depth and surface inductance is $L_s = \mu_0 \lambda_b \coth \lambda_b/t$. For our $\sim 0.5 \mu\text{m}$ thick film we have $L_s \sim 0.82 \text{ pH}$.

The circuit model of the resonator (fig.3, top) has two capacitors (C_1) across either end of a transmission line of characteristic impedance Z_0 , length 2ℓ , and propagation constant $\beta = \omega/v_{ph}$. The resonator made by those three elements is coupled on one end to the readout line through capacitance $C_2 \ll C_1$. By symmetry, there is a virtual ground at the center of the transmission line, so a simpler circuit (fig.3, bottom) can be considered. Resonance occurs when the impedance $Z_C = 1/i\omega C_1$ equals the negative of the input impedance of the shorted transmission line section $Z_{in} = iZ_0 \tan \beta\ell$. At that frequency, the parallel combination of these impedances becomes large and can tune out the large impedance of the small coupling capacitor, producing a short across the readout line (and a dip in its transmission).

From the calculation of capacitance per unit length of the transmission line (\mathcal{C}), the inductance per unit length (\mathcal{L}) and the capacitance of the IDC, for CPS line with a conductor width of $10 \mu\text{m}$ and spacing between conductors of $5 \mu\text{m}$, a resonance frequency of 12 GHz is found, while with sonnet software a frequency

of 5.2 GHz was found. The reason for the disagreement is that the CPS line inductance is quite small and the IDC has a (parasitic) inductance that is significant compared with it. From the IDC capacitance and the simulation result for the resonance frequency, the total inductance of the resonator can be estimated as:

$$L_{res} = \frac{1}{C_1 \omega_{res}^2} = 1.4 \text{ nH}. \quad (1)$$

2.2 Estimated response

The kinetic inductance per unit length of the CPS line is approximately $2L_s/w$, where w is the width of the traces of the CPS line and the factor of two is because there are two traces. This gives $\mathcal{L}_k = 0.16 \mu\text{H}/\text{m}$ and $L_k = \mathcal{L}_k \times 500 \mu\text{m} = 80 \text{ pH}$, while the ratio $\alpha = L_k/L_{res} = 0.057$.

The significant non-fundamental sources of noise are resonator frequency (TLS) noise, which affects only the inductive signal, and amplifier noise, which affects both the inductive and dissipative signals. To minimize the amplifier contribution to the detector noise, we need to optimally couple the resonator to the readout line, which implies that the designed coupling loss, Q_c^{-1} , is equal to the internal loss due to quasiparticles at the peak of the pulse, $Q_{i,qp}^{-1} = \gamma_s S_1(\omega, t) N_{qp} \alpha_{sc} / (2N_0 \Delta V_c)$, γ_s is 0.5 for a thick film in the local limit, $S_1(\omega, t)$ is a Mattis Bardeen factor of order 1, and α_{sc} is found to be 0.15, assuming a penetration depth $\lambda = 500 \text{ nm}$ as found for TiN. We find $Q_c \sim 4 \times 10^4$, which corresponds to a resonator response time of $\tau_r = Q_c / 2\pi f_r \sim 1.3 \mu\text{s}$ and sets the rise time of the detector. The amplifier contribution to the sensitivity, δE_{amp} , can be estimated by considering the smallest resolvable change in transmission amplitude $\delta S_{21}^{amp} = (k_b T_N / 4P_r \tau_{qp})^{1/2}$ for a pulse width of τ_{qp} , determined by the recombination time of the quasiparticles, and a microwave excitation power P_r . Increasing P_r improves the sensitivity, but eventually drives the resonator into a non-linear state due to the current dependence of the kinetic inductance. A photon of energy E_γ produces kE_γ/Δ quasiparticles, where Δ is the gap parameter and k is a material dependent efficiency which accounts for the energy lost to subgap phonon production. k is thought to typically be in the range 0.5–0.7, so we will take the average $k = 0.6$, giving $N_{qp} = 2 \times 10^6$ for a 2 keV photon.

The frequency response of the resonator is given by

$$\frac{\delta f}{f} = \frac{\alpha}{2} \frac{X_s}{X_s(0)} = \frac{\alpha}{2} \gamma_s S_2(\omega, T) \frac{N_{qp}}{2N_0 \Delta V}, \quad (2)$$

where X_s is the surface reactance, V is the volume of the inductor and $S_2(\omega, T)$ is a Mattis-Bardeen factor given by

$$S_2(\omega, T) = 1 + \sqrt{\frac{2\Delta}{\pi k_b T}} \exp\left(-\frac{\hbar\omega}{2k_B T}\right) I_0\left(\frac{\hbar\omega}{2k_B T}\right) \quad (3)$$

Considering $\omega_r/2\pi = 5 \text{ GHz}$, $T \ll T_c$ and $S_2 \approx 4$ we find a fractional frequency shift of $\approx 10^{-5}$. Hence to shift the resonance by a half width, we would want a coupling quality factor $Q_c \sim 5 \times 10^4$. In other units, this sensitivity corresponds to 23 Hz / eV.

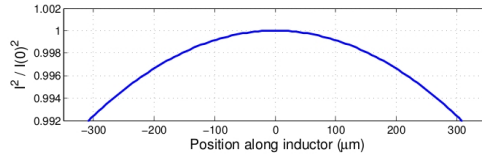


Fig. 4 Distribution of I^2 in the inductor. One part in 1000 uniformity can be expected if the inductor is illuminated over the central 200 microns.

2.3 Response uniformity

The response of the resonator to quasiparticle creation is weighted by the square of the current at the position where the quasiparticles are generated. The current is largest near the shorted end (the virtual ground in the center of the CPS line) and is given by $I = \cos \beta x$, where x is the distance from the center and $\beta = \omega/v_{ph}$. The resonator response is proportional to $I^2(x)$, which is plotted in fig.4.

We will also expect some degradation of the energy resolution if quasiparticles are able to diffuse into the IDCs, where they will produce a very small response. Before they recombine, the quasiparticles will diffuse over a distance of $\zeta \sim \sqrt{D\tau_r}$, where D is the quasiparticle diffusivity and τ_r is the recombination time, so the response shown in the figure will be convoluted with the quasiparticle distribution function. While $\tau_r \sim 10 \mu\text{s}$ is expected for stoichiometric TiN, there is currently no information on D . The measured D for Ta films differs considerably from theory. If we scale results from Ta by the ratio of the normal state conductivities, we might expect D to be around $1 \text{ cm}^2/\text{s}$. With this value, we would have $\zeta \sim 30 \mu\text{m}$. This is the width of a gaussian distribution, so we require that the distance between the photon absorption event and the IDC satisfies

$$\int_0^d dx \frac{1}{\sqrt{2\pi\zeta^2}} e^{-x^2/2\zeta^2} < \Delta E/E = 0.001. \quad (4)$$

Hence, if we illuminate the inductor over its center $200\mu\text{m}$, an insignificant fraction of the quasiparticles will be lost into the capacitors.

Acknowledgements This work is supported by Fondazione Cariplo through the project "Development of Microresonator Detectors for Neutrino Physics".

References

1. F. Low, Journal of the Optical Society of America 51(11), p.1917 (1961).
2. J.J.Bock, Space Science Reviews 74, p.229, (1995).
3. P.K.Day et al., Nature 425, p.817 (2003).
4. J.Gao et al., App. Phys. Lett. 90(10), p.102507 (2007).
5. E. Ferri et al., these proceedings.
6. P.Day, J. Low Temp. Phys. 151(1-2), P.477 (2008).
7. B.A.Mazin, Proc. SPIE 773518 (2010).
8. Noroozian, O., Gao, J., Zmuidzinas, J., LeDuc, H.G., Mazin, B.A., AIP Conf. Proc, 1185, 148, (2009).